Initial eccentricity in deformed ^{197}Au + ^{197}Au and ^{238}U + ^{238}U collisions at $\sqrt{s_{NN}}$ = 200 GeV at the BNL Relativistic Heavy Ion Collider

Peter Filip,[1,*] Richard Lednicky,[2] Hiroshi Masui,[3] and Nu Xu[3]
[1]*Institute of Physics, Slovak Academy of Sciences, 84511 Bratislava, Slovak Republic*
[2]*Joint Institute for Nuclear Research, RU-141980 Dubna, Russia*
[3]*Lawrence Berkeley National Laboratory, Berkeley, California 94705, USA*
(Received 12 September 2009; published 5 November 2009)

Initial eccentricity and eccentricity fluctuations of the interaction volume created in relativistic collisions of deformed ^{197}Au and ^{238}U nuclei are studied using optical and Monte Carlo (MC) Glauber simulations. It is found that the nonsphericity noticeably influences the average eccentricity in central collisions, and eccentricity fluctuations are enhanced from deformation. Quantitative results are obtained for Au + Au and U + U collisions at energy $\sqrt{s_{NN}}$ = 200 GeV.

DOI: 10.1103/PhysRevC.80.054903 PACS number(s): 25.75.Ld, 21.10.Ft

I. INTRODUCTION

Measurement of the elliptic flow [1] and higher-order azimuthal asymmetries [2] in transverse momentum distributions of particles created in relativistic nucleus-nucleus collisions at the BNL Relativistic Heavy Ion Collider (RHIC) [3] provides us with the potential to study collective properties of strongly interacting partonic matter [4]. Hydrodynamical simulations [5] of ultrarelativistic heavy ion collisions at RHIC are often used to determine quantitatively bulk properties of the expanding partonic quantum chromodynamics (QCD) matter created [6]. As an initial condition in hydrodynamical simulations, the asymmetrical shape (eccentricity ε) of the interaction volume of compressed partonic matter must be specified [7].

In collisions of spherical nuclei the geometry of the interaction volume is simply related to the impact parameter and the centrality of collisions [8]. However, in collisions of deformed nuclei, the geometrical orientation of nuclei relative to each other and to the beam axis directly influences initial eccentricity ε as well as the number of binary nucleon-nucleon collisions $N_{\rm coll}$ and the number of participants $N_{\rm part}$ in such collisions. It is important to clarify the influence of nuclear ground-state deformation on the initial conditions in nucleus-nucleus collisions because relativistic interactions of slightly deformed nuclei (Si, Au, Cu, and In) [9] have already been studied at Alternating Gradient Synchrotron (AGS) [10], Super Proton Synchrotron (SPS) [11], and RHIC [12]. Moreover, a precise understanding of the initial geometry of the partonic matter created in ultrarelativistic collisions of heavy prolate nuclei is needed for a reliable interpretation of forthcoming experiments with ^{238}U beams at RHIC. (Colliding heavy prolate nuclei may provide a higher particle density and longer duration in certain configurations.)

The relevance of a slight ground-state deformation of the ^{197}Au nucleus in relativistic Au + Au collisions at RHIC has been discussed only recently [13]. Although electron scattering experiments [14] suggest charge distribution in the ^{197}Au nucleus to be spherical, the nonzero quadrupole moment ($Q = 0.587 \pm 5\%$) is obtained for ^{197}Au from recent hyperfine interaction measurements [15]. Theoretical calculations [9] predict oblate deformation ($\beta_2 = -0.13$) for the ^{197}Au ground state; furthermore, a giant dipole resonance measurement in the ^{197}Au(γ,n) reaction [16] suggests significant oblate ^{197}Au deformation ($|\beta_2| \approx 0.15$).

In this article we study the average eccentricity and eccentricity fluctuations of the interaction volume in collisions of deformed nuclei (^{197}Au and ^{238}U) using optical Glauber [17] and MC-Glauber [18] model simulations.

II. GLAUBER MODEL SIMULATION FOR DEFORMED NUCLEI

The implementation of a deformed nuclear shape in our Glauber model simulations has been done in the following way. A spatial distribution of nucleons has been generated according to the deformed Woods-Saxon density [19]:

$$\rho_w(x, y, z) = \frac{\rho_o}{1 + e^{(r - R_o(1+\beta_2 Y_{20} + \beta_4 Y_{40}))/a}}, \qquad (1)$$

with deformation parameters ($\beta_2 = -0.13, \beta_4 = -0.03$) taken from Ref. [9] for ^{197}Au ($R = 6.38$ fm, $a = 0.53$). For U + U collisions we have used $\beta_2 = 0.28$ in agreement with Ref. [21], and $\beta_4 = 0.093$ was implemented according to Ref. [9]. The deformation parameter β_4 for the ^{238}U nucleus ($R = 6.81$, $a = 0.54$) should be taken into account in U + U simulations because it noticeably influences the shape of the nucleon density in the core of the ^{238}U nucleus. Consequently, the initial conditions of hydrodynamical simulations of U + U collisions depend on the β_4 parameter used. In Fig. 1 we show the transverse profile of the participant nucleon density $\rho_{\rm p}$ obtained using the optical Glauber calculation for the body-body U + U collision (symmetry axes of U nuclei are orthogonal to the beam, collinear, and impact $b = 0$ fm). Although the total eccentricity of participants is only slightly modified assuming $\beta_4 \neq 0$, the eccentricity of the high-density core ($\rho_{\rm p} > \rho_{\rm cut}$) is significantly dependent on β_4 [see Fig. 1(b)]. This can have substantial influence on the

*Peter.Filip@savba.sk

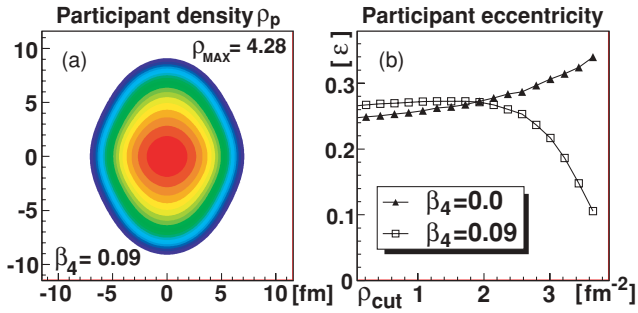

FIG. 1. (Color online) Transverse participant density (a) obtained from the optical Glauber model for body-body U + U collisions using $\beta_2 = 0.28$ and $\beta_4 = 0.093$. (b) shows the participant eccentricity ε of the high-density core ($\rho_p > \rho_{cut}$) for $\beta_2 = 0.28$ and $\beta_4 = 0$ (as used in Ref. [21]) and for $\beta_4 = 0.093$.

elliptic flow strength obtained in hydrodynamical simulations [20].

In our calculations, nuclei have been rotated randomly to simulate unpolarized nucleon-nucleon collisions, which gives the probability distribution $P(\theta) = \sin(\theta)/2$ for polar angles θ_1, θ_2 and the random distribution of azimuthal angles ϕ_1, ϕ_2 (z axis in the beam direction). The optical Glauber model [13] has been used first to clarify the influence of deformation on average eccentricity $\langle\varepsilon\rangle$ and eccentricity fluctuations in Au + Au collisions.

For given orientations of colliding deformed nuclei $\theta_1, \theta_2, \phi_1, \phi_2$ and every given impact parameter b, the density of participants $\rho_{\rm part}(x, y)$ and the density of binary nucleon-nucleon collisions $\rho_{\rm coll}(x, y)$ have been used to calculate participant-weighted $\varepsilon_{\rm part}$ and collisions-weighted $\varepsilon_{\rm coll}$ initial eccentricities [22]:

$$\varepsilon = \frac{\sqrt{\left(\sigma_y^2 - \sigma_x^2\right)^2 + 4\sigma_{xy}^2}}{\sigma_y^2 + \sigma_x^2}, \qquad (2)$$

where $\sigma_x^2 = \langle x^2\rangle - \langle x\rangle^2$, $\sigma_y^2 = \langle y^2\rangle - \langle y\rangle^2$, and the cross term is $\sigma_{xy}^2 = (\langle x \cdot y\rangle - \langle x\rangle\langle y\rangle)^2$ (here denoting $\langle f(x, y)\rangle = \int f(x, y)\rho(x, y)\,dxdy$). Initial eccentricity calculated using Eq. (2) is always a positive number, regardless of the orientation of the deformed overlap shape relative to the impact parameter. This corresponds to the elliptic flow measured in the participant plane [23].

From the total number of participants, $N_{\rm part}$, and binary collisions, $N_{\rm coll}$, the rapidity density of the secondary charged multiplicity $dN_{\rm ch}/d\eta$ can be determined according to the two-component model [24] of particle production:

$$\frac{dN_{\rm ch}}{d\eta} = (1 - X_{\rm hard}) \cdot n_{pp}\frac{N_{\rm part}}{2} + X_{\rm hard} \cdot n_{pp} N_{\rm coll}, \qquad (3)$$

where $X_{\rm hard}$ denotes the fraction of charged multiplicity produced in binary nucleon-nucleon collisions and n_{pp} is the energy-dependent charged multiplicity measured in proton-proton collisions. An initial entropy density $\rho_s(x, y)$ in the transverse plane was evaluated according to the Glauber ansatz [25]:

$$\rho_s(x, y) = \kappa_s[\alpha\rho_{\rm part}(x, y) + (1 - \alpha)\rho_{\rm coll}(x, y)]. \qquad (4)$$

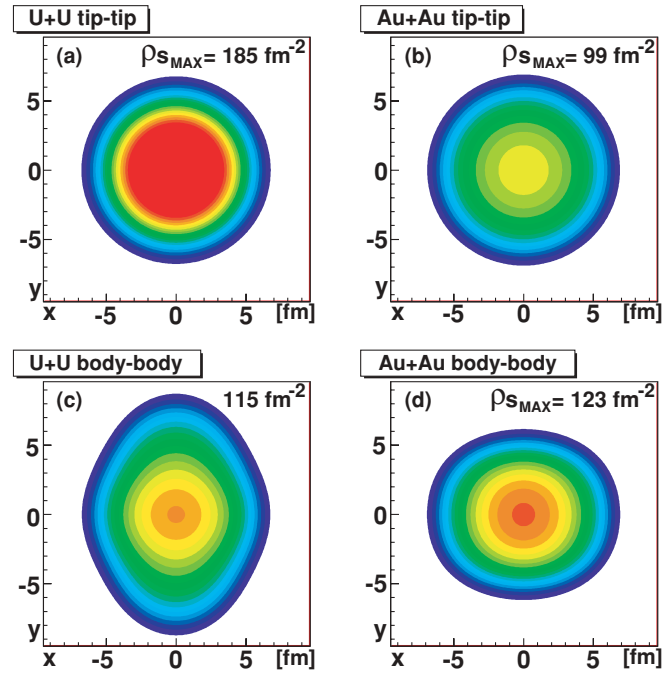

FIG. 2. (Color online) Transverse entropy density for selected orientations in Au + Au and U + U collisions evaluated assuming $\beta_2 = -0.13$, $\beta_4 = -0.03$ for ^{197}Au and $\beta_2 = 0.28$, $\beta_4 = 0.093$ for ^{238}U at energy $\sqrt{s_{NN}} = 200$ GeV.

We use $n_{pp} = 2.49$, $X_{\rm hard} = 0.13$, and $\alpha = 0.75$ for collision energy $\sqrt{s_{NN}} = 200$ GeV. Using parameter $\kappa_s = 14.45$ brings our entropy density calculations into agreement with the results of Heinz and Kuhlman [21].

Transverse entropy density distributions for selected orientations of Au + Au and U + U collisions are shown in Fig. 2. According to expectation, central ($b = 0$) tip-tip oriented U + U collisions (main axes of nuclear ellipsoid parallel to the beam direction) give the highest density of the interacting nuclear matter. It is also clearly observed that the highest entropy densities in Au + Au collisions are obtained in central ($b = 0$ fm) body-body polarized Au + Au collisions (collinear main axes of nuclear ellipsoids are orthogonal to the beam direction). As shown in Fig. 2(d), the initial eccentricity in such collisions is nonzero from the oblate deformation of the ^{197}Au nucleus and the maximum entropy density in such collisions is slightly higher compared to body-body U + U central collisions. The selection of such central Au + Au collisions from the experimental sample of events, however, can be a challenging task.

III. RESULTS AND DISCUSSIONS

The distribution of participant eccentricity $\varepsilon_{\rm part}$ and $dN_{\rm ch}/d\eta$ values obtained from optical Glauber simulation [13] for Au + Au collisions assuming oblate ^{197}Au nuclei (impact parameter $b < 13.6$ fm increased in 0.1-fm steps) is shown in Fig. 3. Nuclear deformation causes variations of eccentricity as well as variations of charged multiplicity $dN_{\rm ch}/d\eta$ at a given fixed impact parameter b from random orientations of deformed nuclei; $\langle\varepsilon\rangle$ can then be calculated as the mean value

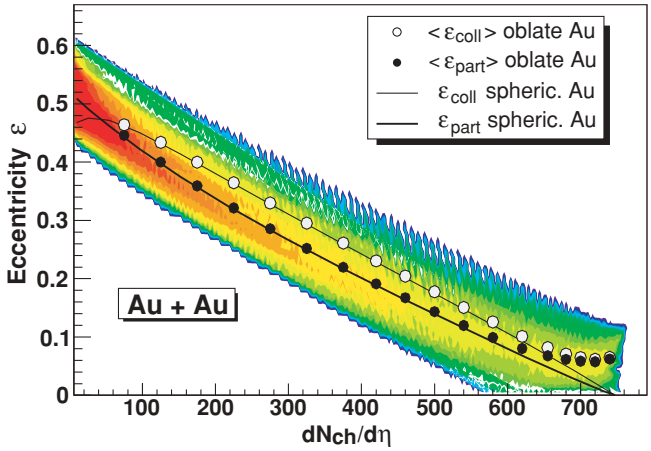

FIG. 3. (Color online) Distribution $\{\varepsilon_{\rm part};\, dN_{\rm ch}/d\eta\}$ from the optical Glauber simulation for Au + Au ($\beta_2 = -0.13$) collisions at energy $\sqrt{s_{NN}} = 200$ GeV. The average participant eccentricity $\langle\varepsilon_{\rm part}\rangle$ at given $dN_{\rm ch}/d\eta$ is indicated by black dots. Solid lines starting at $dN_{\rm ch}/d\eta = 740$ represent $\varepsilon_{\rm part}$ and $\varepsilon_{\rm coll}$ for the spherical ($\beta_2 = 0$) Au + Au simulation. Open circles indicate average $\langle\varepsilon_{\rm coll}\rangle$ values from the $\{\varepsilon_{\rm coll};\, dN_{\rm ch}/d\eta\}$ distribution (not shown).

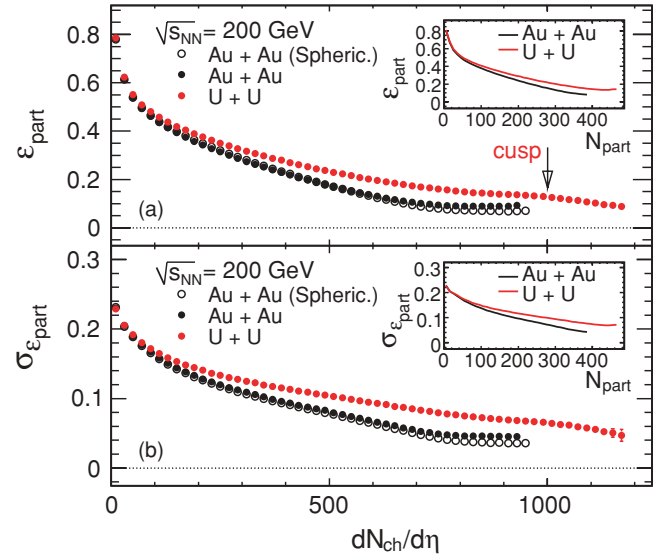

FIG. 4. (Color online) Average eccentricity $\varepsilon_{\rm part}$ and width of eccentricity fluctuations σ_ε as a function of charged particles multiplicity $dN_{\rm ch}/d\eta$ within $|\eta| < 0.5$ obtained from the MC-Glauber simulation for Au + Au and U + U collisions.

of eccentricities at a given interval of multiplicity $dN_{\rm ch}/d\eta$ (indicated by solid black circles in Fig. 3). For spherical nuclei, the single eccentricity $\varepsilon_{\rm part}$ and charged multiplicity $dN_{\rm ch}/d\eta$ value are obtained for a given impact parameter in the optical Glauber simulation (indicated by the solid line in Fig. 3). This happens because there are no fluctuations of participant eccentricity from the individual positions of interacting nucleons (at a given impact parameter b) in the optical Glauber model. Also, $dN_{\rm ch}/d\eta$ does not fluctuate at fixed b in the optical Glauber simulation of spherical nuclei collisions. (For spherical nuclei $\varepsilon \to 0$ for $b = 0$.)

It is observed that the deformation of colliding nuclei affects the average eccentricity in the most central collisions. Highest multiplicities are obtained for body-body orientations of ^{197}Au nuclei. In such collisions the eccentricity is enhanced from the nonspherical shape of the ^{197}Au nucleus. Consequently, the average eccentricity $\langle\varepsilon\rangle$ in very-high-multiplicity Au + Au collisions is increased because of the oblate ground-state deformation of ^{197}Au.

In MC-Glauber simulations, the eccentricity fluctuations originating from individual positions of interacting nucleons are mixed together with eccentricity fluctuations from the deformation of nuclei. The width of the fluctuations from a finite number of interacting nucleons $\sigma_\varepsilon = \sqrt{\langle\varepsilon^2\rangle - \langle\varepsilon\rangle^2}$ and width σ_β of fluctuations from deformation of nuclei are added in quadrature, and the resulting width of eccentricity fluctuations is

$$\sigma_\varepsilon = \sqrt{\sigma_\beta^2 + \sigma_\varepsilon^2}. \tag{5}$$

In Fig. 4 we show the charged multiplicity dependence of the average eccentricity $\langle\varepsilon\rangle$ obtained for deformed Au + Au and U + U collisions. Results obtained assuming the ^{197}Au nucleus to be spherical are also shown. Identical Woods-Saxon density parameters are used in our optical and MC-Glauber simulations.

Fluctuations of participant eccentricity from a finite number of interacting nucleons are rather large and it is mainly in central collisions where the influence of ground-state deformation [see Eq. (5)] is visible in Au + Au collisions. For central U + U collisions we observe a cusp in the average eccentricity dependence on charged particle multiplicity $dN_{\rm ch}/d\eta$. This behavior is a consequence of the effective self-orientation of U + U high-multiplicity collisions: only U + U collisions with an oriented tip-tip configuration contribute to the region of highest multiplicities. In such collisions the initial eccentricity is reduced because the transverse profile of longitudinally oriented U nuclei is spherical. The cusp predicted in Fig. 4 for the initial eccentricity is a consequence of the binary-collisions-generated contribution to the multiplicity $dN_{\rm ch}/d\eta$ in Eq. (3).

This behavior agrees well with the results of optical Glauber simulations [26] if the two-component model of particle production [24] is used to calculate $dN_{\rm ch}/d\eta$.

Experimentally, one measures the elliptic flow strength v_2 and elliptic flow fluctuations width σ_{v_2} at a given collision centrality characterized by $dN_{\rm ch}/d\eta$. Whether the cusp predicted in Fig. 4 for U + U collisions appears in the elliptic flow dependence on multiplicity $dN_{\rm ch}/d\eta$ remains to be verified at RHIC. Assuming hydrodynamical expansion for the compressed QCD matter created in ultrarelativistic collisions of heavy nuclei, one can assume $v_2 = \lambda\langle\varepsilon\rangle$, $\sigma_{v_2} = \lambda\sigma_\varepsilon$ (in Ref. [20] the factor $\lambda \approx 0.25$) and, consequently, $\sigma_\varepsilon/\langle\varepsilon\rangle \approx \sigma_{v_2}/v_2$. This allows one to compare the $\sigma_\varepsilon/\langle\varepsilon\rangle$ value directly with the experimentally measured ratio σ_{v_2}/v_2.

One may expect that an eventual sudden deviation of the experimental value σ_{v_2}/v_2 from the MC-Glauber evaluated ratio $\sigma_\varepsilon/\langle\varepsilon\rangle$ studied as a function of particle multiplicity $dN_{\rm ch}/d\eta$ could be a signal of the phase transition of QCD matter created in relativistic nucleus-nucleus collisions. This might happen because of the simultaneous increase of σ_ε fluctuations and

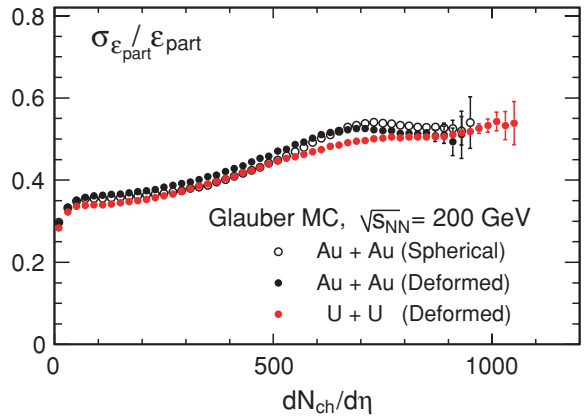

FIG. 5. (Color online) Ratio $\sigma_\varepsilon/\langle\varepsilon\rangle$ obtained from the MC-Glauber simulation for Au + Au and U + U collisions as a function of centrality measured by $dN_{\rm ch}/d\eta$.

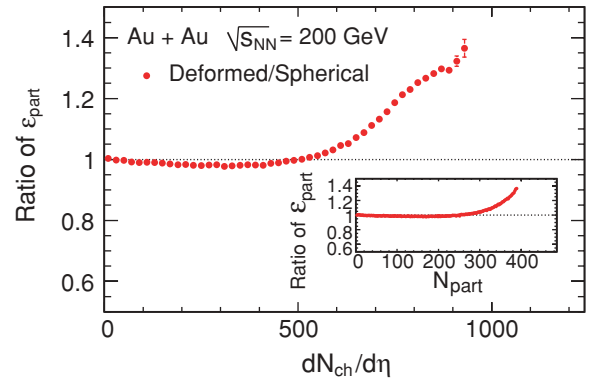

FIG. 6. (Color online) Ratio of average eccentricities obtained from the MC-Glauber simulation for Au + Au collisions assuming the oblate and spherical ground state of the ^{197}Au nucleus.

softening of the equation of state of thermalized QCD matter at the phase transition.

The ratio $\sigma_\varepsilon/\langle\varepsilon\rangle$ for collisions of ^{197}Au and ^{238}U nuclei obtained from our MC-Glauber simulation is shown in Fig. 5. One observes different behavior for central Au + Au and central U + U collisions. For Au + Au collisions the ratio $\sigma_\varepsilon/\langle\varepsilon\rangle$ becomes saturated and slightly decreases at $dN_{\rm ch}/d\eta > 700$, whereas in U + U collisions the ratio shows a continuous increase even for high $dN_{\rm ch}/d\eta$.

When the ratio $\sigma_\varepsilon/\langle\varepsilon\rangle$ is evaluated (in the Glauber model simulation) as a function of the number of participating nucleons, Au + Au and U + U collisions do not exhibit distinct differences. It is the number of binary nucleon-nucleon interactions $N_{\rm coll}$ that changes significantly in tip-tip and body-body U + U central ($b \approx 0$ fm) collisions. Consequently, deformation effects show up in the eccentricity behavior mainly when the multiplicity $dN_{\rm ch}/d\eta$ [see Eq. (3)] is used to quantify the collision centrality.

One observes from Fig. 6 that the average eccentricity $\langle\varepsilon\rangle$ in Au + Au collisions is influenced significantly in central collisions, if ^{197}Au oblate deformation is taken into account. The most central bin of Au + Au collisions at RHIC, therefore, deserves a more detailed study. For example, the average eccentricity $\varepsilon_{\rm part}$ (and measured elliptic flow strength v_2) in the highest-multiplicity collisions of oblate ^{197}Au nuclei (see Fig. 4) might show a very small increase at maximal $dN_{\rm ch}/d\eta$ if the fraction of body-body Au + Au collisions (with parallel orientations of nuclear ellipsoid axes) is effectively enhanced [e.g., by requiring the minimal spectator signals in zero-degree calorimeters (ZDCs)]. However, because of fluctuations of multiplicity $dN_{\rm ch}/d\eta$ and fluctuating signals of spectators in ZDCs, the result of such attempts is not guaranteed.

In noncentral collisions ($dN_{\rm ch}/d\eta < 500$ in Fig. 6), we observe only a small decrease of the average eccentricity if the oblate shape of the ^{197}Au nucleus is assumed. Bulk properties of the partonic matter created at RHIC inferred from the comparison with hydrodynamical calculations of noncentral collisions [5] are thus only slightly affected.

To summarize, we have studied the average eccentricity and eccentricity fluctuations in collisions of deformed nuclei using optical and MC-Glauber simulations. We observe increased eccentricity fluctuations in collisions of deformed nuclei and increased (up to 30%) average eccentricity for central deformed Au + Au collisions. In central collisions of prolate nuclei we predict a cusp-like behavior of the average eccentricity if studied as a function of centrality determined by multiplicity $dN_{\rm ch}/d\eta$. We think that taking into account the nonsphericity of the ^{197}Au nucleus and the β_4 parameter for ^{238}U is necessary for the precise understanding of the initial state of the expanding partonic matter created at RHIC. We suggest that from the comparison of the experimentally measured ratio (σ_{v_2}/v_2) and the ratio $(\sigma_\varepsilon/\langle\varepsilon\rangle)$ obtained in MC-Glauber simulations one can obtain information on changes in the behavior of partonic matter. This can be an additional tool in the search for a critical point at RHIC.

ACKNOWLEDGMENTS

The authors are grateful to Art Poskanzer for his comments. This work was supported by the US Department of Energy under Contract No. DE-AC03-76SF00098, Slovak Grant Agency for Sciences VEGA under Grant No. 2-7116-29, and JINR Dubna.

[1] J.-Y. Ollitrault, Phys. Rev. D **46**, 229 (1992).
[2] P. F. Kolb, Phys. Rev. C **68**, 031902(R) (2003).
[3] J. Adams *et al.*, Nucl. Phys. **A757**, 102 (2005).
[4] H.-T. Elze and U. Heinz, Phys. Rep. **183**, 81 (1989).
[5] M. Luzum and P. Romatschke, Phys. Rev. C **78**, 034915 (2008); H.-J. Drescher, A. Dumitru, C. Gombeaud, and J.-Y. Ollitrault, *ibid.* **76**, 024905 (2007); D. Teaney, *ibid.* **68**, 034913 (2003).
[6] M. J. Tannenbaum, Rep. Prog. Phys. **69**, 2005 (2006).
[7] W. Broniowski, M. Chojnacki, W. Florkowski, and A. Kisiel, Phys. Rev. Lett. **101**, 022301 (2008).
[8] W. Broniowski and W. Florkowski, Phys. Rev. C **65**, 024905 (2002).
[9] P. Möller, J. R. Nix, W. D. Myers, and W. J. Swiatecki, At. Data Nucl. Data Tables **59**, 185 (1995).

[10] T. Abbott *et al.*, Phys. Rev. Lett. **70**, 1393 (1993).
[11] R. Arnaldi *et al.*, Phys. Rev. Lett. **96**, 162302 (2006).
[12] G. Wang *et al.*, Nucl. Phys. **A774**, 515 (2006).
[13] P. Filip, Phys. Atom. Nucl. **71**, 1609 (2008).
[14] B. Hahn, D. G. Ravenhall, and R. Hofstadter, Phys. Rev. **101**, 1131 (1956).
[15] W. M. Itano, Phys. Rev. A **73**, 022510 (2006).
[16] C. Nair *et al.*, Phys. Rev. C **78**, 055802 (2008).
[17] A. Bialas, M. Bleszynski, and W. Czyz, Nucl. Phys. **B111**, 461 (1976).
[18] M. L. Miller, K. Reygers, S. J. Sanders, and P. Steinberg, Annu. Rev. Nucl. Part. Sci. **57**, 205 (2007); J. Hüfner and J. Knoll, Nucl. Phys. **A290**, 460 (1977).
[19] K. Hagino, N. W. Lwin, and M. Yamagami, Phys. Rev. C **74**, 017310 (2006).
[20] P. F. Kolb, J. Sollfrank, and U. Heinz, Phys. Rev. C **62**, 054909 (2000).
[21] A. Kuhlman and U. Heinz, Phys. Rev. C **72**, 037901 (2005).
[22] B. Alver *et al.*, Phys. Rev. Lett. **98**, 242302 (2007).
[23] J.-Y. Ollitrault, A. M. Poskanzer, and S. A. Voloshin, Phys. Rev. C **80**, 014904 (2009).
[24] D. Kharzeev and M. Nardi, Phys. Lett. **B507**, 121 (2001).
[25] P. F. Kolb, U. Heinz, P. Huovinen, K. J. Eskola, and K. Tuominen, Nucl. Phys. **A696**, 197 (2001).
[26] P. Filip, in *Proceedings of the 16th Conference of Czech and Slovak Physicists, Hradec Králové, Czech Republic, 2008*, edited by J. Kříž (MAFY, Hradec Králové, 2009), pp. 66–72.